Extended Virtual-Flux Decoupling Hysteresis Control for Mains Connected Three-Level NPC Inverter Systems

L. A. Serpa and J. W. Kolar

Swiss Federal Institute of Technology
Power Electronic Systems Laboratory
ETH Zentrum / ETL H16, Physikstrasse 3
CH-8092 Zurich / SWITZERLAND
serpa@lem.ee.ethz.ch

***Abstract* – An extended approach which adapts the Virtual-Flux Decoupling Hysteresis Control initially employed for the conventional two-level VSI to a three-level NPC inverter is proposed in this paper. To extract the benefits of this topology, namely low output harmonic distortion and lower switches blocking voltage, the classical single-band hysteresis strategy must be modified and the balance of the mid-point potential have to be guaranteed. The mid-point voltage is controlled by influencing the zero sequence current generated in the decoupling loop. The method is adapted to be used with an LCL output filter, where some undesirable characteristics, such as filter resonance, have to be compensated. Theoretical analysis is presented and the performance of the proposed method is verified by simulation.**

***Index Terms*—Decoupling Hysteresis, Grid Connected, Three-Level NPC.**

I. Introduction

Since its introduction in 1981 [1], the three-level neutral-point clamped (NPC) voltage source inverter (Fig. 1) has demonstrated some advantages over the conventional two-level inverter. It has been applied in medium and high power applications due to the inherent advantages, namely: voltage across the switches is clamped to half of the dc-link, produces low output voltage and current harmonic distortion and reduces the dv/dt stress on the load.

The most widely used control system for three-level inverters is the Space Vector Modulation (SVM). This method produces an output voltage and current with low harmonic distortion, even at low switching frequency. It also permits the possibility of controlling the mid-point voltage. However, it suffers from a low dynamic performance and is affected by the stability requirements of the feedback loop.

An alternative approach to regulate the power flow in a three-level NPC inverter is to use hysteresis comparison to determine the switching instants of each phase [2][3]. As with all hysteresis systems, this approach would be expected to have fast and robust response. On the other hand it produces a variable switching frequency and coupling between phases exist when applied to three-phase, three-wire systems. In this case the phase current does not only depend on the corresponding applied voltage but also on the current in the other two phases. To minimize this interference the decoupling hysteresis control has been proposed [4][5]. It generates a more uniform switching pattern and allows a near constant switching frequency by modulating the hysteresis boundaries. Making use of these properties, a sensorless mains voltage, power control with almost constant switching frequency for a two-level voltage source inverter, called Virtual-Flux Decoupling Hysteresis Control (VF-DHC), was proposed in [6]. The virtual-flux concept permits the estimation of the grid voltage avoiding the derivative term required to calculate the voltage drop across the output filter inductor.

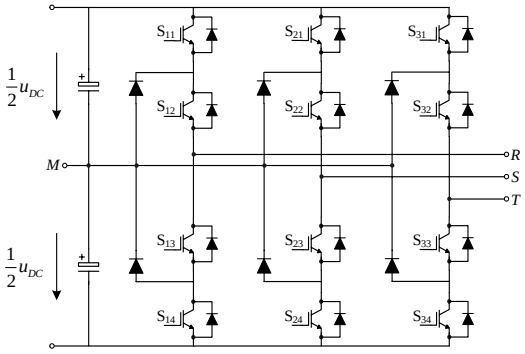

Fig. 1. Three-Phase Three-Level NPC Voltage Source Inverter.

This paper extends the VF-DHC to be used with a three-level NPC inverter. To take full advantage of this topology some aspects of the VF-DHC approach must be reviewed. In Section II the main idea of the virtual-flux decoupling hysteresis control applied to a two-level VSI is presented. The resulting switching performance is showed to be similar to the classical PWM scheme, however with the dynamic response inherent to the hysteresis approach. The adapted VF-DHC is proposed in Section III. The classical single-band hysteresis strategy is replaced in order to allow the selection of three distinct levels generated by NPC inverters and the mid-point potential is regulated by controlling the zero sequence component. The proposed approach is proved by simulation in Section IV and extended for high power application, where usually a third order filter is employed, in Section V. Extra control loops must be added in order to compensate undesirable characteristic inherent in LCL filters. Finally, Section VI verifies the extended method with LCL filter by simulation.

II. VF-Decoupling Hysteresis Control

The virtual-flux decoupling hysteresis controller (VF-DHC) proposed in [6] (Fig. 2) has the same basic structure as the standard hysteresis control, where the phase current is subtracted from a current reference and the hysteresis controller generates a switching signal from the current error. However, the coupling between phases inherent in three-phase, three-wire inverters is avoided by employing the decoupling strategy. Reducing this phase current interaction results in the switching frequency becoming more uniform and allows for a near

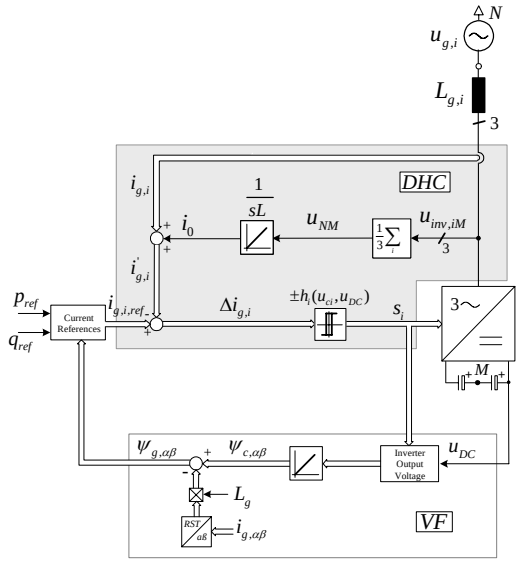

Fig. 2. Virtual-Flux Decoupling Hysteresis Control (VF-DHC) structure.

constant switching frequency if a variable hysteresis band is implemented.

To reduce the number of voltage sensors the virtual-flux (VF) concept is used. It extracts the mains voltage from the dc voltage, switching state and grid currents.

From the desired active and reactive powers and the estimated grid virtual-flux, the current references in the stationary reference frames are calculated using

$$i_{\alpha,ref} = \frac{2}{3}\frac{\psi_{g,\alpha}\cdot q_{ref} - \psi_{g,\beta}\cdot p_{ref}}{\omega\cdot\left(\psi_{g,\alpha}^2+\psi_{g,\beta}^2\right)} \quad (1)$$

$$i_{\beta,ref} = \frac{2}{3}\frac{\psi_{g,\alpha}\cdot p_{ref} + \psi_{g,\beta}\cdot q_{ref}}{\omega\cdot\left(\psi_{g,\alpha}^2+\psi_{g,\beta}^2\right)} \quad (2)$$

The phase quantities are then obtained by a stationary coordinates transformation and controlled by a current hysteresis control.

A. Virtual-Flux

An estimation of the grid voltage can be obtained by subtracting the voltage across the filter inductor from the inverter output voltage. However, this approach has the drawback that the current is differentiated and noise in the current signal is gained through the differentiation. To prevent this, the Virtual-Flux (VF) method was proposed in [7]. The VF strategy assumes that the line voltage and the ac-side inductors are quantities related to a virtual ac motor. Making an analogy with ac motors, R_g and L_g (Fig. 3) represent respectively the

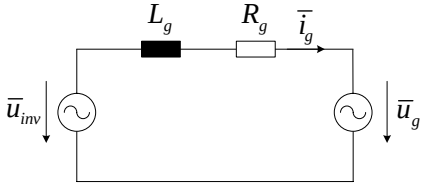

Fig. 3. Equivalent circuit of a grid connected three-phase VSI with L output filter.

stator resistance and the stator leakage inductance and the line voltage u_g, represents the machine's electro-motive force.

The grid virtual-flux calculation is based on flux definition (3) and the voltage loop equation (4)

$$\bar{\psi}_g = \int \bar{u}_g \cdot dt \quad (3)$$

$$\bar{u}_g = \bar{u}_{inv} - R_g\cdot\bar{i}_g - L_g\cdot\frac{d\bar{i}_g}{dt} \quad (4)$$

Neglecting the series resistance of the line inductor, the grid virtual-flux can be calculated based on the measured grid current and the inverter output voltage

$$\bar{\psi}_g = \int \bar{u}_{inv}\cdot dt - L_g\cdot\bar{i}_g \quad (5)$$

where the inverter output voltage can be calculated based on the dc-link voltage and the converter switching states.

B. Decoupling Strategy

The decoupling controller has an additional control loop that generates the current control signal, i_0. By summing the measured line current, $i_{g,i}$ with i_0, a virtual current $i'_{g,i}$ is formed. With the correct formation of i_0 the switching of the hysteresis controller can occur without any interaction between each of the phase controllers. The phase interaction is caused because the DC bus mid-point to neutral voltage is not constant, as it is dependent on each of the inverter output voltages.

In the case where *M*, the mid-point of the DC capacitors is not connected to the mains neutral *N*, the current is not only dependent on the respective inverter output voltage but is also influenced by the zero sequence voltage u_{MN}.

$$L_g\frac{di_{g,i}}{dt} = u_{inv,iM} - u_{g,i} - u_{MN} \quad (6)$$

where the zero sequence voltage is given by

$$u_{MN} = \frac{1}{3}\left(u_{inv,RM} + u_{inv,SM} + u_{inv,TM}\right). \quad (7)$$

Therefore, combining the equations (6) and (7), the coupling between phases is clearly seen from

$$L_g\frac{di_{g,i}}{dt} = u_{inv,iM} - u_{g,i} - \frac{1}{3}\left(u_{inv,RM} + u_{inv,SM} + u_{inv,TM}\right) \quad (8)$$

In order to eliminate the interaction between phases, an additional current term, i_0, is added into the current controller ($i'_{g,i} = i_{g,i} + i_0$, cf. Fig. 2). The current signal, i_0, is generated by integrating either the calculated voltage u_{MN} given by (7) or the measured zero sequence voltage u_{MN} as given by

$$i_0 = \frac{1}{L_g}\int u_{MN}\, dt \quad (9)$$

The VF-DHC behavior is observed in the experimental results showed in Fig. 4. Although the basic control scheme is based on the conventional hysteresis controller, the addition of the decoupling loop makes the behavior similar to the PWM. The spectrum becomes centered around the switching frequency Fig. 4(b) and the switching frequency over one cycle is almost constant Fig. 4(c).

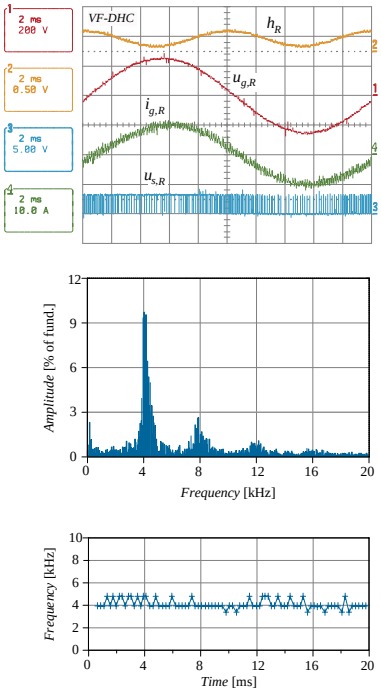

Fig. 4. Experimental performance of the VF-DHC with switching frequency of 4kHz for a two-level VSI. The resulting mains current $i_{g,R}$ and respective gate signals $u_{sw,R}$ (a), frequency spectrum (b) and switching frequency behavior during one fundamental cycle (c).

III. VF-DHC FOR THREE-LEVEL NPC INVERTER

To utilize the benefits of a three-level inverter, such as less harmonic contend and lower blocking voltage of switching devices, the classic VF-DHC (Fig. 2) previously employed for two-level system must be modified.

The basic difference in a three-level inverter is that three voltage levels can be applied to each phase, namely: $+u_{DC}/2$ (switching on the two upper switches S_{11} and S_{12}), 0 (switching on the two central switches S_{12} and S_{13}) and $-u_{DC}/2$ (switching on the two lower switches S_{13} and S_{14}). Therefore, to increase or decrease the line voltage, there are more possibilities than in a two-level inverter. However, it requires a modified hysteresis modulation, which replaces the conventional single-band hysteresis.

Another important aspect which differs from the two-level approach and must be respected to ensure a correct operation of the three-level inverter is the balancing of the dc-link mid-point potential. If this condition is not fulfilled, the advantages before mentioned are no longer valid because the harmonic distortion increases rapidly and some individual switches have to support a higher blocking voltage.

Therefore, to adapt the existing VF-DHC to operate with a three-level NPC inverter, these features mentioned, namely switching strategy and mid-point voltage control, must be included. Fig. 5 shows the extended VF-DHC scheme. The main idea of controlling the grid current through a hysteresis control and the decoupling strategy is maintained. The estimated virtual-flux and the desired active and reactive powers generate the current references to be compared with the measured current $i_{g,i}$ added to zero sequence current i_0. However, to allow the selection of three voltage levels a three-level modulation is implemented by replacing the conventional single-band hysteresis by double-band hysteresis.

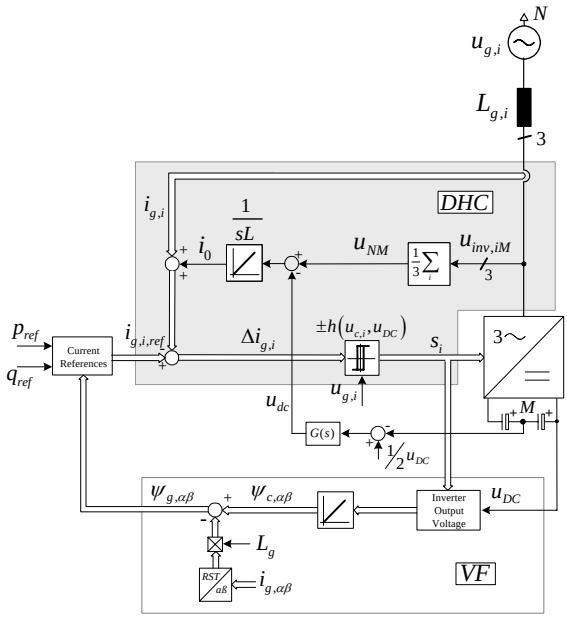

Fig. 5. Extended VF-DHC structure for three-level NPC inverter.

A. Hysteresis Strategy

As mentioned, the decoupling control strategy avoids the switching interaction between phases which results in a more uniform switching frequency. Besides that, it allows a near constant frequency by modulating the hysteresis band.

The modulated hysteresis band also differs from the two-level approach. In the two-level the inverter output voltage can only switch between plus and minus dc-link voltage. However, in the three-level case during the positive mains cycle, the inverter output voltage can reach either half of the dc-link voltage or zero. While at the negative cycle it can be either zero or negative half of the dc-link voltage.

To derive an expression for the variable hysteresis band, the positive grid cycle is considered. When the two upper switches are in on state the output voltage is $+u_{DC}/2$ and the voltage across the filter inductor is the difference between half of the dc-link and the grid voltage. The current error decreases until the lower hysteresis band is reached. At the time the two central switches are conducting, the inverter output voltage is zero and the current error increases until it reaches the upper hysteresis band. Together these two switching times represent one switching cycle which is given by

$$T = \frac{2 \cdot h \cdot L_g \cdot \frac{u_{DC}}{2}}{u_{inv}\left(\frac{u_{DC}}{2} - u_{inv}\right)} \qquad (10)$$

Rearranging (10) the hysteresis band required to produce a near constant switching frequency is expressed as

$$h(t) = \frac{u_{inv}(t) \cdot \left(\frac{u_{DC}}{2} - u_{inv}(t)\right)}{2 \cdot L_g \cdot f_{sw} \cdot \frac{u_{DC}}{2}} \qquad (11)$$

The shape of the hysteresis band for one half of a mains period is shown in Fig. 6.

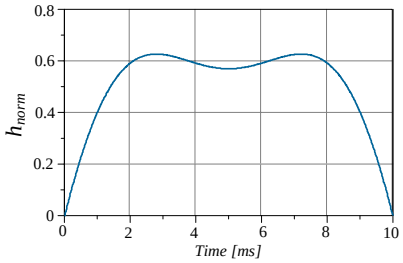

Fig. 6. Normalized hysteresis band shape for one half of mains period.

In addition the classical single-band hysteresis does not permit the selection of three distinct levels generated by the NPC inverter. An alternative is to use a double-band hysteresis strategy to detect an out-of-bounds current error.

The basic principle of the double-band hysteresis control is shown in Fig. 8. When the current exceeds the inner hysteresis boundary, the next higher (or lower) voltage level should be selected in order to ensure a single switch commutation to the new inverter state. However, this new inverter state may not be adequate to force the current error to begin to return to zero. In this case the current error continuous in the same direction until reach the outer hysteresis boundary. At this point the inverter should switch to the next higher (or lower) voltage level to bring the current error to operate again between the inner hysteresis bands.

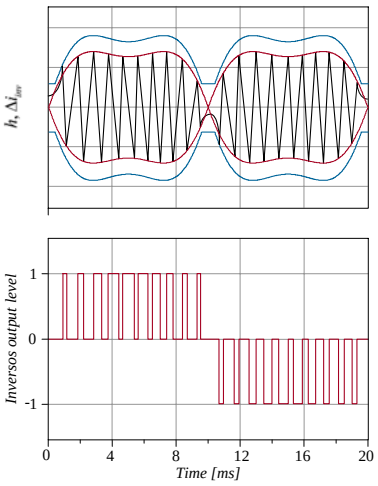

Fig. 8. Double-Band hysteresis strategy for three-level inverter.

B. Mid-Point Voltage Control

The variation in the mid-point potential is a problem inherent in the NPC inverter topology. An excessive high voltage may be applied to switching devices when the mid-point (*M*) potential varies from the center potential of the dc-link voltage.

Various strategies have been presented to balance the mid-point voltage. The majority of the *M* voltage balancing schemes rely on some form of manipulation of the redundant vectors presents in the three-level topology. Basically, the relative duration of these vectors in a pair is usually adjusted in order to compensate for any deviation of the mid-point potential.

An illustration of the effect caused by redundant switching states (0 -1 -1) and (1 0 0) in the mid-point current can be seen in Fig. 7. Although the line-to-line voltages produced by both switching states are identical ($u_{RS}=u_{DC}/2$, $u_{ST}=0$ and $u_{TR}=-u_{DC}/2$), the generated zero sequence output voltages are different.

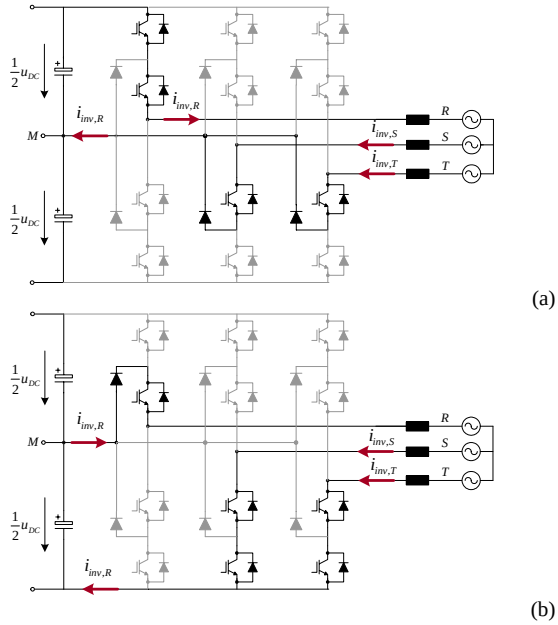

Fig. 7. Influence caused by the redundant vector in the mid-point current during a (a) positive small vector (0 -1 -1) and (b) negative small vector (1 0 0).

Assuming positive current in the phase *R* and negative current in the phases *S* and *T*, the mid-point current flows out of the mid-point when the state (0 -1 -1) is selected (Fig. 7(a)). In this case the upper capacitor is charged and the lower capacitor is discharged. An opposite effect on the capacitors voltages is observed when the state (1 0 0) is chose, since the mid-point current now flows into the mid-point, as shown in Fig. 7(b). Therefore, although the NPC inverter generates the same voltage vector in both cases, the direction of the mid-point current differs, owing to the zero sequence output voltage. This shows that the zero sequence voltage plays an important role in the potential variation [8].

In [9] the principle of balancing the mid-point voltage by controlling the zero sequence component for the specific case of hysteresis control is described. Since in the hysteresis method the control signals are generated directly from the difference between reference and actual value of each phase current according to the hysteresis boundaries, the possibility of controlling the mid-point voltage by influencing the frequency of each redundant state is limited basically to a modification of the reference value shape. Therefore, since the amplitude and shape of the currents references are given by the power requirements, the only degree of freedom consists of the addition of a zero-component i_0.

In the proposed VF-DHC, the zero sequence current is created by adding the signal from the voltage controller to the input of the integrator, as showed in Fig. 5. The voltage controller compares the voltage across the lower capacitor against a reference (12), which is normally half of the total dc-link voltage, and a proportional controller produces a dc voltage u_{dc} from the error (13).

$$\Delta u = u_{C_{l,ref}} - u_{C_l} \tag{12}$$

$$u_{dc} = k_p \cdot \Delta u \tag{13}$$

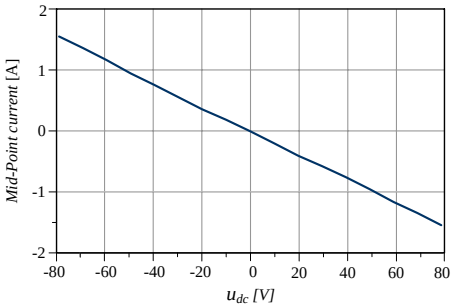

Fig. 9. Transfer characteristic from the controlling signal u_{dc} to the average mid-point current.

The influence of the voltage controller output u_{dc} on the average mid-point current is shown in the Fig. 9

This clearly shows that for example, if the lower capacitor voltage u_{C_l} is bellow the reference voltage $u_{C_{l,ref}}$, the resulting positive controller output voltage u_{dc}, produces a negative average mid-point current, which charges the lower capacitor, controlling the mid-point potential.

IV. Simulation Results

In order to verify the effectiveness of the proposed VF-DHC for three-level NPC inverter, simulations have been performed. The output inductance of 18mH links between the inverter and the grid (400V / 3-phase). The inverter, designed to operate with an average switching frequency of 2.5kHz, is supplied by an 800V DC power source.

The improvement in the switching pattern is clearly observed by comparing the performance of the classical hysteresis control and the proposed decoupling strategy as shown in Fig. 10. The grid currents (Fig. 10(a)) and inverter output voltage (Fig. 10(b)) generated by the conventional hysteresis control show long periods where no switching occurs due to the interaction between phases. Adding the zero sequence current i_0 to the measured currents, the switching instants showed on the grid currents (Fig. 10(e)) and the inverter output voltage (Fig. 10(f)) becomes more uniform. The switching performance is better observed on the resulting current spectrum (Fig. 10(g)) which becomes more centered around 2.5kHz and the instantaneous switching frequency measured at the two upper switches (Fig. 10(h)) that are maintained almost constant.

The influence of the zero sequence component on the mid-point potential is observed in Fig. 11. By injecting a zero sequence current proportional to the dc link voltage deviation, the balance of the dc-link voltages can be achieved (Fig. 11(b)). Moreover, the overshoot can be reduced when comparing against the balancing obtained by using the classical hysteresis control (Fig. 11(a)).

V. VF-DHC for High Power Application

The proposed VF-DHC system can be adapted to be used with a third order LCL output filter and therefore achieve reduced levels of harmonic distortion for a VSI operating with a low switching frequency. The LCL filter attenuates the switching ripple substantially and the overall size of the LCL filter is reduced compared to only an L filter. However, systems incorporating LCL filter requires extra control effort in order to compensate some undesirable characteristics such as the filter resonance.

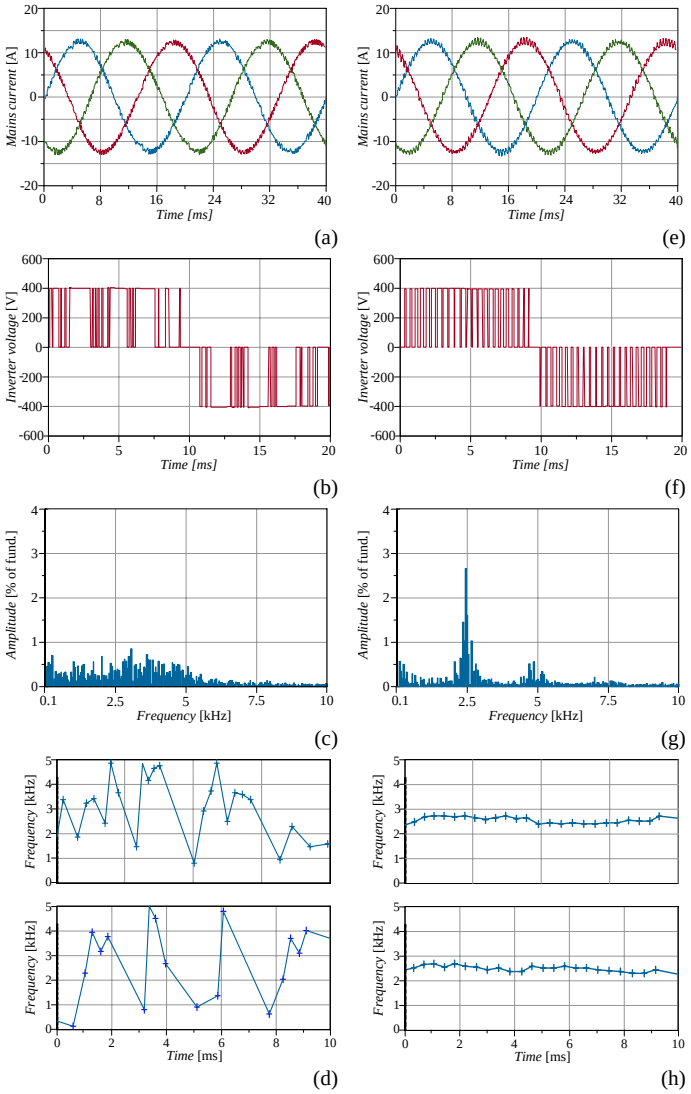

Fig. 10. Simulation results of mains current, inverter output voltage, harmonic spectrum and instantaneous switching frequency (a), (b), (c) and (d) provided by conventional hysteresis control (e), (f), (g) and (h) with the decoupled approach.

The modified VF-DHC showed in Fig. 12 maintains the core of the conventional approach and incorporates outer control loops which damp the filter resonance, reject the influence of grid voltage harmonics [10][11] and compensate for the reactive power of the capacitor, since the active and reactive power are controlled on the inverter side.

Since the switching states are selected via hysteresis control, there is no modulation index or common control signal within

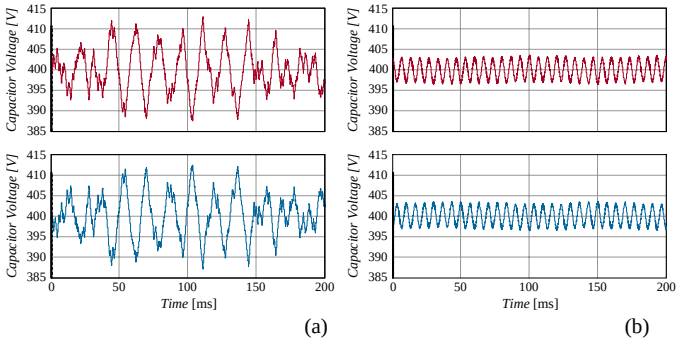

Fig. 11. Simulation results of voltages across the dc-link capacitors (a) with conventional hysteresis control and (b) with the decoupling method.

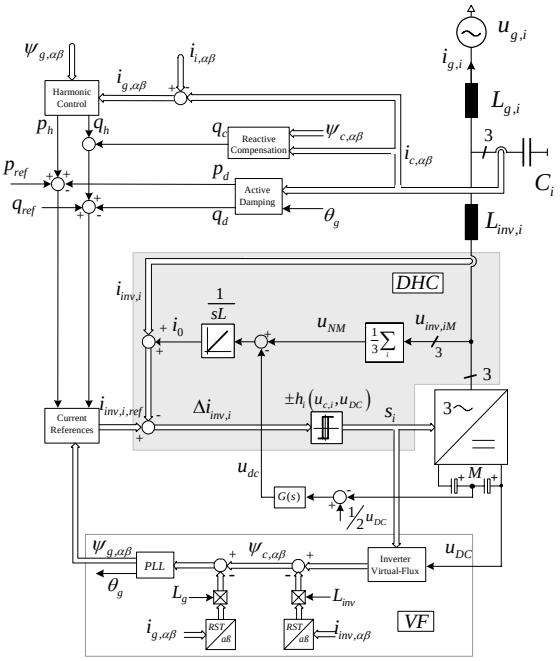

Fig. 12. Extension of the VF-DHC for high power application where LCL filter is usually employed.

the control loops where outer loops control signal can be directly added. To overcome this limitation the active damping control, as well as the individual harmonic rejection control have to be implemented by acting directly on the active and reactive power components. These control signals have to be added to the fundamental references (p_{ref} and q_{ref}).

The active damping strategy can be applied effectively because the resonance frequency of the output filter is usually inside the bandwidth of the inverter control loops. The active damping is achieved by emulating a resistor in parallel with the filter capacitor by creating a current source proportional to the capacitor voltage resonance component.

The harmonic control block proposed in [10][11] regulates the harmonics individually in their respective individual synchronous reference frame. Each harmonic quantity to be controlled is transformed into its own individual synchronous reference frame. The corresponding harmonic quantities appear as dc in their own reference frame, consequently a PI control is enough to guarantee zero steady state error.

VI. Simulation Results for the Extended Approach

To confirm the efficacy of the extended VF-DHC with an LCL output filter, simulations have been carried out. The setup consists of a 6kW NPC inverter, with an averaged switching frequency of around 2.5kHz, connected to a controlled 400V - 50Hz 3-phase AC power source via an LCL filter (L_{inv}=17mH, L_g=5.6mH and C=18µF).

The oscillation caused by the filter resonance is reduced when the active damping loop is added to the conventional VF-DHC approach, as can be seen comparing the grid current (Fig. 13(a),(c)) and the respective current harmonic spectrum (Fig. 13(b),(d)) for the conventional and extended method.

VII. Conclusion

An extension of the conventional VF-DHC to be used with a three-level NPC inverter has been presented in this paper. Different hysteresis strategy as well a mid-point potential

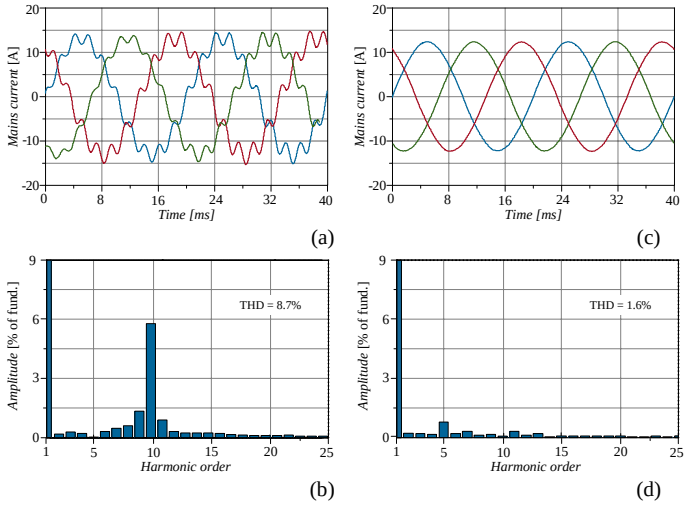

Fig. 13. Simulation results of mains current and respective harmonic spectrum (a)-(b) provided by conventional VF-DHC and (c)-(d) when the active damping approach and harmonic rejection control loops are added to the main VF-DHC.

control are incorporated to the conventional VF-DHC in order to utilize the full advantages of three-level topology. The method is also adapted to be used with a third order LCL filter by adding active damping and harmonic control strategies. The proposed controller behavior is investigated by simulation.

References

[1] A. Nabae, I. Takahashi and H. Akagi, "A new neutral-point-clamped PWM inverter," *IEEE Trans. Ind. Applicat.*, vol. 17, pp. 518-523, Sept./Oct. 1981.

[2] M. Marchesoni, "High-Performance Current Control Techiniques for Applications to Multilevel High-Power Voltage Source Inverters," *IEEE Trans. Power Electron.*, vol. 7, pp. 189-204, Jan. 1992.

[3] A. Bellini, S. Bifaretti and S. Costantini, "A New Approach to Hysteresis Modulation Techiniques for NPC Inverters," *in Proc. ISIE'02*, vol. 3, July 2002, pp. 844-849.

[4] L. Malesani, P. Mattavelli and P. Tomasin, "Improved Constant-Frequency Hysteresis Current Control of VSI Inverters with Simple Feedforward Bandwidth Prediction," *IEEE Trans. Ind. Applicat.*, vol. 33, no5, pp. 1194-1201, Sep./Oct. 1997.

[5] L. Dalessandro, U. Drofenik, S.D. Round and J.W. Kolar, "A Novel Hysteresis Current Control for Three-Phase Three Level Rectifiers," *in IEEE Proc. APEC'05*, vol.2, Mar. 2005, pp. 501-507.

[6] L. A. Serpa, S. D. Round and J. W. Kolar, "A Virtual-Flux Decoupling Hysteresis Current Controller for Mains Connected Inverter Systems," *in IEEE Proc. PESC'06*, Jun. 2006, pp.1-7.

[7] M. Malinowski, M. J. Jasinski and M.P. Kazmierkowski, "Simple Direct Power Control of Three-Phase PWM Rectifier Using Space-Vector Modulation (DPC-SVM)," *IEEE Trans. Ind. Applicat.*, vol. 51, no. 2, pp. 447-454, April 2004.

[8] S. Ogasawara and H. Akagi, "Analysis of Variation of Neutral Point Potential in Neutral-Point-Clamped Voltage Source PWM Inverter," *in IEEE Proc.IAS'93*, vol. 2, Oct. 1993, pp. 965-970.

[9] J. W. Kolar, U. Drofenik and F. Zach, "Space Vector Based Analysis of the Variation and Control of the Neutral Point Potential of Hysteresis Current Controlled Three-Phase/Switch/Level PWM Rectifier Systems," *in Proc. PEDS'95*, vol. 1, Feb. 1995, pp. 22-33.

[10] L. A. Serpa, S. Ponnaluri, P. M. Barbosa and J.W. Kolar, "A Modified Direct Power Control Strategy Allowing the Connection of Three-Phase Inverter to the Grid through LCL Filters," *in Proc. IAS'05*, vol. 1, Oct. 2005, pp. 565-571.

[11] S. Ponnaluri and A. Brickwedde, "Overriding Individual Harmonic Current Control with fast dynamics for Active Filtering," *in Proc. PESC'01*, June 2001, pp. 1596-1601.